An Analytical DC– and AC–Model for Vertical Smart Power DMOS Transistors

M. Stiftinger and S. Selberherr
Institute for Microelectronics, Technical University of Vienna
Gusshausstrasse 27–29, A-1040 Vienna

Smart Power MOS transistors serve primarily as an interface between digital control logic and the power load. Since they are also used in analog applications there are high demands on the accuracy of analytical models for circuit simulation. The approach for a physically based analytical model for vertical DMOS (double-diffused MOS) transistors which will be presented in this paper accounts for non-uniform channel doping-concentration in lateral direction, for space-charge limited current in the drift region and is able to describe the behavior of the device by means of a single formula. Our model is supported by two-dimensional numerical device simulations using BAMBI [1].

The channel doping-profile of the n-channel vertical DMOS transistor (see Fig. 1) is defined by the different lateral diffusions of p-base and n^+-source and is approximated by an exponential shape: $N_A(x) = N_A(0)\exp\left(-\eta\frac{x}{L}\right)$. The model describing the channel is based on a continuous MOS-model [2]. Integrating the drain-current in the strong inversion regime along the channel

$$I_D = -W\mu_{eff}E_x(x)q_C(x) = -W\mu_{eff}q_C(x)\frac{dU_C}{dx} \tag{1}$$

with the electric field in x-direction $E_x(x) = \frac{dU_C}{dx}$ and the channel charge-density $q_C(x)$ yields under the assumtion of a linear distribution of the channel-voltage ($U_C \simeq U_{DSeff}x/L$) [3]:

$$I_D = \frac{W}{L_{eff}}\mu_{eff}C_{ox}\left(U_{GSeff}(\eta) - \frac{1 + F1\,C_{dB}(\eta)/C_{ox}}{2}U_{DSeff}\right)U_{DSeff} \tag{2}$$

For $\eta = 0$ the "classical" result is obtained: $U_{GSeff}^{classical} = U_{GS} - U_{FB} - 2\Phi_F + 2\frac{C_{dB}^{classical}}{C_{ox}}(2\Phi_F - U_{BS})$ in the strong inversion regime and $C_{dB}^{classical} = F2\sqrt{\frac{\epsilon qN_A(0)}{2(2\Phi_F - U_{BS})}}$. In the weak inversion regime U_{GSeff} is independent of η: $U_{GSeff} \propto \exp\left(\frac{U_{GS}-U_{th}}{2U_t}\right)$. Fig. 3 compares the values of U_{GSeff} from the enhanced and the "classical" model: $\left(U_{GSeff}(\eta) - U_{GSeff}^{classical}\right)/N$ (where N is given by $N = 2\frac{C_{dB}^{classical}}{C_{ox}}(2\Phi_F - U_{BS})$) and $C_{dB}(\eta)/C_{dB}^{classical}$ as functions of η. $\eta > 0$ leads to a higher drain-current than in the "classical" case which results from an increased channel conductance

due to the smaller bulk charge at the drain end of the channel. C_{dB} can be regarded as derivative of the bulk charge-density with respect to the channel potential.

The assumption of a linear distribution of the channel-voltage allows the consideration of the nonuniform channel doping when integrating Equ. (1). The approach in [3] integrates Equ. (1) neglecting the nonuniform channel doping but calculates C_{dB} seperately (also under the assumption of a linear distribution of the channel-voltage) so that the nonuniform channel doping is accounted for. Besides that the results of our approach seem to be more physically sound it allows also an analogous consideration of η in the derivation of the MOSFET charges for a charge-based capacitance model.

The capacitance model is derived analogously to [4]. The formulae for the charges assigned to the four contacts of the device read:

$$Q_D = -WL\frac{\int_0^{U_{DS}} q^2 n^2(U_C) \int_0^{U_C} qn(U_C')\, dU_C' dU_C}{\left(\int_0^{U_{DS}} qn(U_C)\, dU_C\right)^2} \tag{3}$$

$$Q_S = -WL\frac{\int_0^{U_{DS}} q^2 n^2(U_C) \left(\int_0^{U_{DS}} qn(U_C')\, dU_C' - \int_0^{U_C} qn(U_C')\, dU_C'\right) dU_C}{\left(\int_0^{U_{DS}} qn(U_C)\, dU_C\right)^2} \tag{4}$$

$$Q_B = -WLC_{ox}\left(\gamma\sqrt{2\Phi_F - U_{BS}}\,\frac{2}{\eta}\left(1-\exp\left(-\frac{\eta}{2}\right)\right) + \kappa f_B \frac{\int_0^{U_{DS}} U_C \exp\left(-\frac{\eta}{2}\frac{x}{L}\right) qn(U_C)\, dU_C}{\int_0^{U_{DS}} qn(U_C)\, dU_C}\right) \tag{5}$$

with

$$qn(U_C) = C_{ox}\left(U_{GS} - U_{FB} - 2\Phi_F - U_C(x) - f_B \exp\left(-\frac{\eta}{2}\frac{x}{L}\right)\left(2(2\Phi_F - U_{BS}) + \kappa U_C(x)\right)\right) \tag{6}$$

Φ_F, f_B and γ are given by

$$\Phi_F = U_T \ln\frac{N_A}{n_i} \tag{7}$$

$$\gamma = \frac{\sqrt{2\epsilon_s q N_A}}{C_{ox}} \tag{8}$$

$$f_B = \frac{\gamma f_c}{2\sqrt{2\Phi_F - U_{BS}}} \tag{9}$$

The above equations are integrated under the assumption of $U_C(x) \approx U_{DS}\frac{x}{L}$.

The gate charge can be calculated from the fact that the sum of all four terminal charges must be zero. The capacitances are are defined as partial derivatives of the charges with respect to the terminal voltages:

$$C_{ij} = \delta_{ij} \frac{\partial Q_i}{\partial U_j}, \tag{10}$$

with

$$\delta_{ij} = \begin{cases} 1 & : \quad i = j \\ -1 & : \quad i \neq j \end{cases} \tag{11}$$

For $\eta = 0$ this enhanced model leads to the "classical" form of a charge–based capacitance model.

Because of the nonuniform lateral channel doping the carriers reach the saturation velocity at the source side of the channel. Therefore the channel-charge distribution is almost constant along the channel and is not influenced by the nonuniform doping. In conformity with this fact Q_D and Q_S for the enhanced model differ only slightly from the "classical" model. The nonuniform channel doping has only influence on Q_B and Q_G. Fig. 4 shows $Q_B/Q_B^{classical}$ over η.

Device simulations show that the current in the drift region is space-charge limited (Fig. 5 and Fig. 6). A first approach is to model this by a simple JFET-model. This leads to a subcircuit model (Fig. 2) in which the source contact of the JFET is connected to the drain contact of the MOSFET describing the channel in an internal node which is "located" at the drain end of the channel. The space-charge is mainly controlled by the voltage between the p-base of the DMOS and the internal node between drift region and channel [5]. This concept has been improved with our more sophisticated model instead of the simple JFET-model.

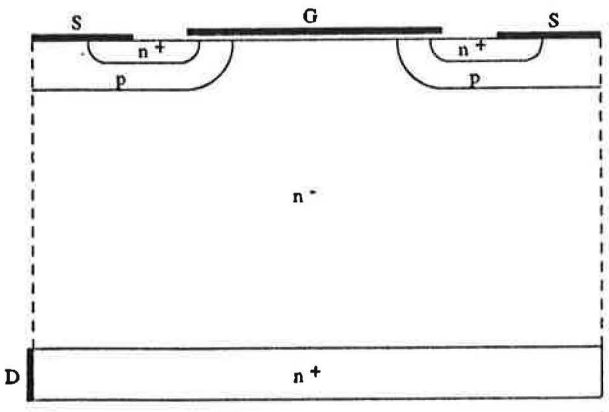

Fig.1. Structure of the vertical DMOS transistor.

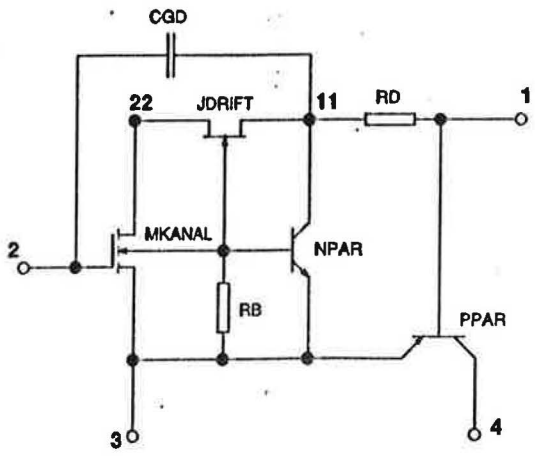

Fig.2. Subcircuit DMOS Model.

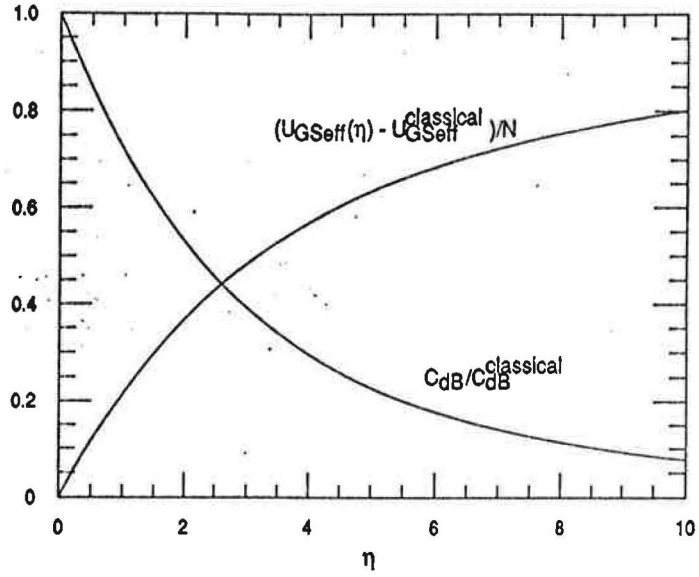

Fig.3. $\left(U_{GSeff}(\eta) - U_{GSeff}^{classical}\right)/N$ and $Q_{dB}(\eta)/C_{dB}^{classical}$ over η.

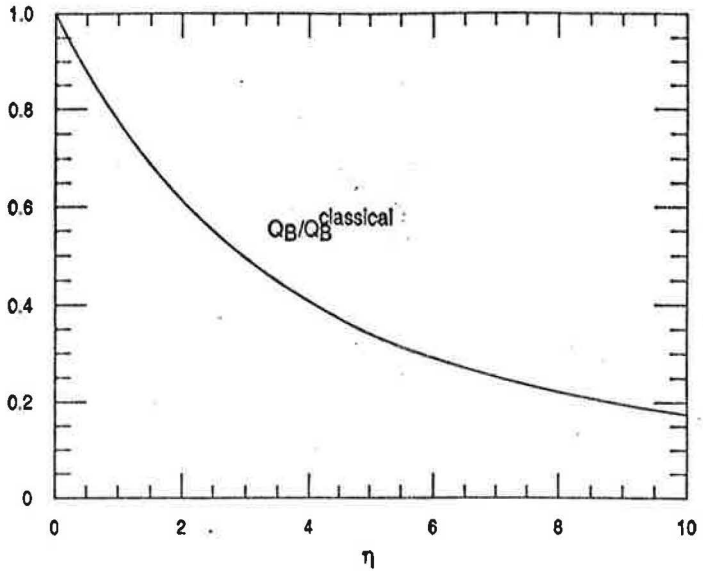

Fig.4. $Q_B/Q_B^{classical}$ for $U_{DS} = 1V$, $U_{GS} = 5V$ and $U_{BS} = 0V$.

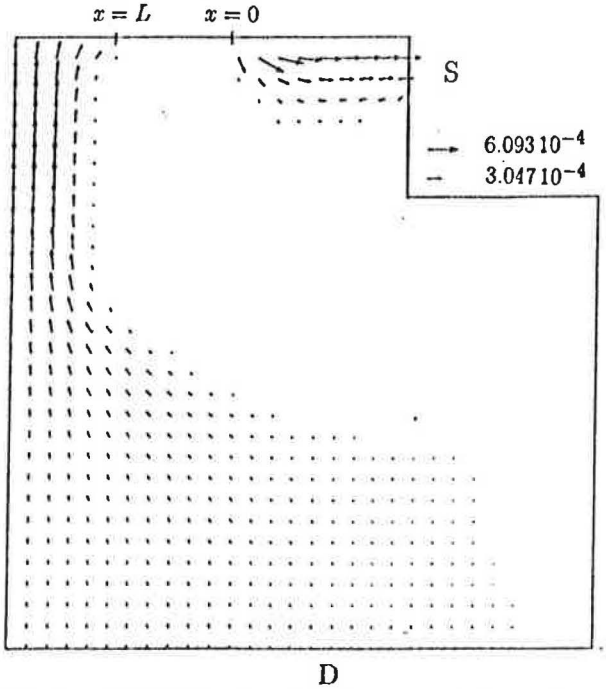

Fig.5. BAMBI-simulated current flow lines for $U_{GS} = 10V$ and $U_{DS} = 5V$.

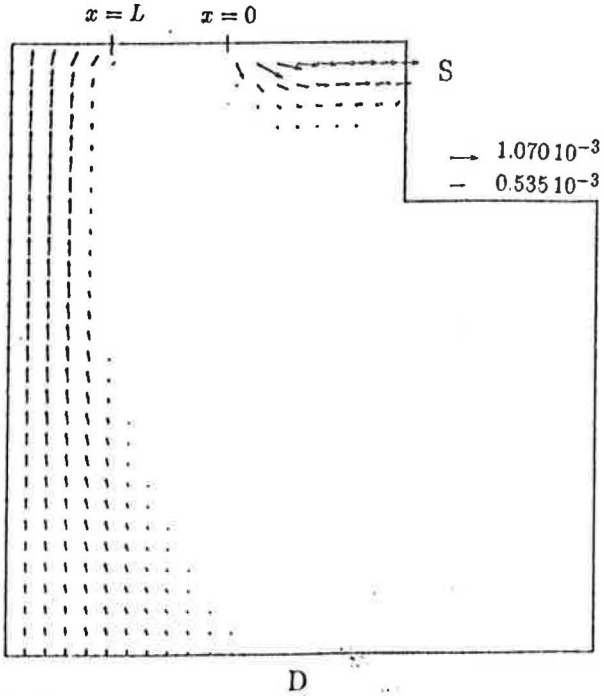

Fig.6. BAMBI-simulated current flow lines for $U_{GS} = 10V$ and $U_{DS} = 35V$.

Acknowledgement

This work is supported by the Development Center for Microelectronics, SIEMENS EZM, Villach, Austria, and by SIEMENS AG, Munich, Germany

References

[1] A.F. Franz, G.A. Franz, W. Kausel, G. Nanz, P. Dickinger, C. Fischer, "BAMBI 2.1 User's Guide", *Technical University Vienna*, 1989.

[2] U. Claeßen, G.E. Müller-L., B. Lemaître, H.L. Zapf, "Erhöhte Genauigkeit bei der Simulation analoger CMOS-Schaltungen durch ein verbessertes MOS-Kompaktmodell", *AEÜ*, Vol. 44, No. 2, pp. 139–147, 1990.

[3] Y.-K. Kim, J.G. Fossum, "Physical DMOST Modeling for High-Voltage IC CAD", *IEEE Trans.Electron Devices*, Vol. 37, No. 3, pp. 797–803, March 1990.

[4] S. Oh, D. E. Ward, R. W. Dutton, "Transient Analysis of MOS Transistors", *IEEE J. Solid-State Circuits*, vol. SC-15, no. 4, pp. 797–803, August 1980.

[5] W. Soppa, "Stand der Modellierung von Vertikal-DMOSFET's in Smart-Power-Mischtechnologie", *Internal Rep., SIEMENS HL CAD 31*, München, September 1990.